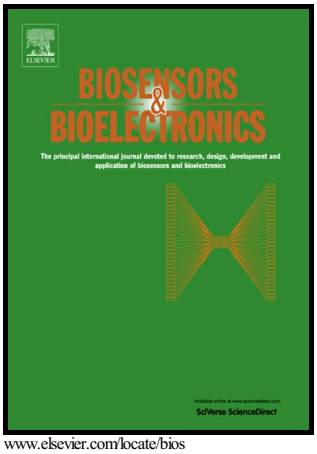

www.elsevier.com/locate/bios

Immunosensing procedures for carcinoembryonic antigen using graphene and nanocomposites

John H.T. Luong, Sandeep Kumar Vashist

PII: S0956-5663(15)30606-0
DOI: http://dx.doi.org/10.1016/j.bios.2015.11.053
Reference: BIOS8183

To appear in: *Biosensors and Bioelectronic*

Received date: 28 September 2015
Revised date: 29 October 2015
Accepted date: 17 November 2015

Cite this article as: John H.T. Luong and Sandeep Kumar Vashist, Immunosensing procedures for carcinoembryonic antigen using graphene and nanocomposites, *Biosensors and Bioelectronic* http://dx.doi.org/10.1016/j.bios.2015.11.053

Immunosensing procedures for carcinoembryonic antigen using graphene and nanocomposites

John H.T. Luong [a*] *and Sandeep Kumar Vashist* [b,c*]

[a]Innovative Chromatography Group, Irish Separation Science Cluster (ISSC), Department of Chemistry and Analytical, Biological Chemistry Research Facility (ABCRF), University College Cork, Cork, Ireland.

[b]Institute of Clinical Chemistry and Pathobiochemistry, Klinikum Rechts der Isar der Technische Universität München, Ismaninger Str. 22, D-81675 Munich, Germany.

[c] Present address: Micro/Nanophysics Research Laboratory, RMIT University, Melbourne, VIC 3001, Australia.

*****Corresponding authors' E-mail: j.luong@ucc.ie and sandeep.vashist@tum.de; sandeepkumar.vashist@rmit.edu.au

Abstract

Two-dimensional (2D) graphene, sp^2-hybridized carbon, and its two major derivatives, graphene oxide (GO) and reduced graphene oxide (rGO) have played an important role in immunoassays (IAs) and immunosensing (IMS) platforms for the detection of carcinoembryonic antigen (CEA), an implicated tumor biomarker found in several types of cancer. The graphene family with high surface area is functionalized to form stable nanocomposites with gold nanoparticles (AuNPs) and electron mediators. The capture anti-CEA antibody (Ab) with high density can be anchored on AuNPs of such composites to provide remarkable detection sensitivity, significantly below the level found in normal subjects and cancer patients.

Electrochemical and fluorescence/chemiluminescence-quenching properties of graphene-based nanocomposites are exploited in various detection schemes. Future endeavors are envisioned for the development of an array platform with high-throughput for CEA together with other tumor biomarkers and C-reactive protein, a universal biomarker for infection and inflammation. The ongoing efforts dedicated to the replacement of a lab-based detector by a cellphone with smart applications will further enable cost-effective and frequent monitoring of CEA in order to establish its clinical relevance and provide tools for real-time monitoring of patients during chemotherapy.

Keywords

graphene, graphene oxide, reduced graphene oxide, carcinoembryonic antigen, immunoassay, immunosensing platform, electrochemical sensing, chemiluminescence, fluorescence quenching.

Introduction

IAs using polyclonal or monoclonal antibody (Ab) serve as a workhorse in analytical, clinical, forensic, and environmental monitoring for the detection of biomarkers, protein/enzyme, DNA, tumor cells, viruses, small molecules, etc. with remarkable detection sensitivity and selectivity. Conventional IAs are based on the binding of capture Ab (cAb) to a typical polystyrene-based microtiter plate (MTP) to capture a target antigen to form an immunocomplex (IMC). Both simple adsorption and covalent binding strategies are employed for the immobilization of cAb on the pristine or modified MTP surface. Among various detection schemes, this IMC is often allowed to form a tertiary complex with a detection antibody (dAb), a format known as a

sandwich assay. The dAb is pre-conjugated with a fluorescence dye, an electroactive species, gold nanoparticles (AuNPs), silver nanoparticles (AgNPs), quantum dots, etc. to enable the binding event's quantitation. The dAb can also be labeled with an enzyme, known as enzyme-linked immunosorbent assays (ELISA), where its reaction with a corresponding substrate can be monitored and quantified by different detection procedures. The confinement of cAb on a sensing chip or an electroactive surface form the basis for the development of electrochemical (EC) or optical IMS biosensing. Accordingly, bioelectrocatalysis of H_2O_2 and the luminol/H_2O_2 chemiluminescence reaction catalyzed by labeled horseradish peroxidase (HRP) are often used due to their simplicity, high detection sensitivity and reliability (Huang and Ren, 2011).

2D graphene, sp^2-hybridized carbon, has emerged recently as a nanoscale material with high surface area and other important properties including excellent electrical conductivity and a small band gap (Geim, 2009). Electronic properties of graphene have been discussed widely in the literature (Peres et al, 2006) and will not be addressed here. In graphene, the sp^2-orbitals form three strong covalent bonds to the nearest neighbors, resulting in its extraordinary mechanical strength. The remaining π-electron per atom is delocalized over the graphene planar surface, which is in turn responsible for electrical conductivity. Such electrons can travel large distances without being scattered, rendering it a promising nanomaterial for fast electronic components (Neto et al, 2004).

Biocompatibility of graphene-based materials has also received considerable attention due to their potential applications in biomedicine, biosensing and tissue engineering (Pinto et al, 2013). Although detailed and longer-term studies for toxicities of graphene and its related materials are needed for *in vivo* biomedical graphene applications, graphene has been widely used in biosensing and analytical sciences. This material can be used to modify the surface of an MTP or

a sensing chip/electrode to accommodate very high biomolecule loadings to improve detection sensitivity and other bioanalytical parameters. There are considerable advances in the synthesis and characterization of graphene, GO and reduced graphene oxide (rGO), hereafter defined as the graphene family. Of notice is the fabrication of the high-quality sheets of few-layer graphene via chemical vapor deposition (CVD) on thin nickel films (Rafiee et al, 2012). Graphene-based electrodes exhibit superior electrocatalysis over carbon nanotubes (CNTs) (Alwarappan et al, 2009) and significantly lower charge-transfer resistance compared to graphite and glassy carbon (GC) materials (Zhou et al, 2009). The graphene family also forms nanocomposites with polymers, conducting polymers, electron mediators, biomolecules, surfactants, and other nanomaterials including quantum dots and metal nanoparticles (Hu et al, 2014, Premkumar and Geckeler, 2012). Negatively charged GO with ionic groups and aromatic domains bind dyes, electroactive molecules and charged proteins via electrostatic as well as π-π stacking interactions. Such nanocomposites can be patterned on a substrate and exploited in IAs and diversified biosensing platforms with excellent analytical performance.

This review aims to unravel the role, current pending technical issues and future feasibility of this fascinating 2D nanomaterial in various IA formats and detection schemes for the detection of CEA, an important tumor marker for colorectal and other types of cancer.

General features of graphene

Among several literature procedures, CVD on metallic surfaces would lead to the synthesis of single, few, or multilayer graphene. Graphene nanoplatelets (GNPs) are also commercially available in a granular form with an average thickness of 6-10 nm and various sizes up to 50 microns. The MTP is made of hydrophobic polystyrene, a long carbon chain with pendant benzene rings on every alternate carbon. Hence, a non-treated MTP surface should interact

strongly with the graphene family via hydrophobic interaction to form a stable layer with an enhanced surface area. To date, the graphene family has been widely used for surface modification by drop-casting of a graphene material dispersed in organic solvents on the sensing interface. For multi-analyte detection with high-throughput, ELISA plates with 96 wells or higher density are commercially available and readily usable in various optical detection schemes. Electrodes can be embedded in the well bottom of such plates for electrochemical analysis in an array. The benzene ring of the polystyrene-based MTP lends itself to chemical modification/ radiation to form amine and carboxyl groups. Other reactive groups, N-hydroxysuccinimide, maleimide and hydrazide groups, can also be grafted onto a polystyrene surface via a photo-linkable spacer arm. The resulting slightly ionic, hydrophobic surfaces with high binding capacities exhibit hydrophobic as well as ionic interactions with GO or rGO to form a stable interface layer for the subsequent modification, bioconjugation, and immunosensing. A regular array of GO sheets can also be patterned at a localized site on a microscope slide or a similar substrate (Figure 1). The fabrication procedure involves both negatively charged GO with COOH groups and positively charged GO with amine NH_2 groups, as the latter can be prepared by surface functionalization with ethylenediamine via the well-known EDC reaction. COOH-GO adheres on the aminated-glass slide with an opposite charge by electrostatic attraction. An array of multilayer thin films is fabricated by alternate layer by layer application of the two GO suspensions (Jung et al, 2013).

Insert Figure 1 here

As a prerequisite for surface modification and bioconjugation, GNPs must be dispersed as a stable suspension in order to exploit their optimal properties including high surface areas ranging from 300-750 m^2 g^{-1}. However, due to significant π–π interactions, GNPs cannot be stabilized as a concentrated mixture regardless of the preparation method. The dispersion of GNPs will cease once the suspension attains a threshold electrical resistance regardless of the time and power used for sonication. In general, smaller GNPs are dispersed more effectively than their bigger counterparts, and low viscous matrices provide a better dispersion with ultrasonication. Among various attempted solvents and surfactants (Table 1A), the most popular for this purpose are *N*-methylpyrrolidone (NMP) and an expensive ionic liquid, which only result in 2.1 mg mL^{-1} (Alzari et al, 2011) and 5.33 mg mL^{-1} (Nuvoli et al, 2011), respectively, of dispersed GNPs. Other novel graphene solvents offer better dispersion compared to NMP (Table 1B).

Of interest is the use of 3-aminopropyltriethoxysilane (APTES), a simple silane, to disperse hydrophobic graphene to form a suspension (Vashist et al, 2014). The graphene modified MTP provides a significant increase in the surface area to accommodate high biomolecule loadings. The APTES-NH_2 group is then readily crosslinked with the free NH_2 of the capture antibody by glutaraldehyde activation. Alternatively, the APTES-NH_2 wrapped on MTP and GNPs can be crosslinked with the cAb-COOH groups via EDC activation. After modification, the solvent must be removed from the resulting interface as required for the subsequent bioconjugation steps. Therefore, NMP with a high boiling point of 205 °C compared to 56 °C for acetone is difficult to evaporate from the interface. Similarly, noncovalent modification of graphene with a small organic molecule might exhibit inherent electrochemistry or optical property, non-specific binding and/or interference with the subsequent bioconjugation step.

GO can be readily prepared by chemical exfoliation of graphite in fuming nitric acid (Brodie, 1859), whereas the preparation of highly oxidized GO requires a concentrated sulfuric acid and fuming nitric acid mixture (Staudenmaier, 1898) or $KMnO_4$ and $NaNO_3$ in concentrated H_2SO_4 (Hummers Jr and Offeman, 1958). The C–O bond in GO disrupts the sp^2 conjugation of the hexagonal graphene lattice, rendering GO an insulator. A GO suspension is more stable in water compared to pristine graphene due to the presence of oxygen-containing groups. GO contains a large amount of oxygen functional groups including carboxyl groups, which form amide bonds with amino-terminated biomolecules. GO binds dyes, charged proteins, hydrophobic molecules via combined electrostatic and π-π stacking interactions. This feature can be exploited for facilitated bioconjugation and novel detection schemes as GO retains near-infrared, visible and ultraviolet fluorescence properties (Dreyer et al, 2010). The chemistry of GO has been widely discussed in the literature (Dreyer et al, 2010) and will not be repeated here. In brief, GO is nonconductive electrically and very defective, but can be treated with a reducing agent, e.g., hydrazine or EC reduction (Chng and Pumera, 2011), known as rGO with enhanced conductivity and electrical properties. Both GO and rGO are more soluble in deionized water (6.6 and 4.74 mg L^{-1}, respectively), and most soluble in *N*-methyl-2-pyrrolidone (NMP), 8.7 and 9.4 mg L^{-1}, respectively. Similar solubility is noted for rGO in *O*-dichlorobenzene (8.91 mg L^{-1}) and 1-chloronaphthalene (8.1 mg L^{-1}), however, GO is less soluble in these two solvents (1.91 and 1.8 mg L^{-1}). The dispersion behavior of GO and rGO in 18 common solvents including deionized water has been investigated by Konios et al. (2014).

In general, both graphene and rGO are advocated in EC detection schemes to modify electrode materials, whereas GO plays an important role in an optical measurement platform with fluorescence or chemiluminescence detection. Also of interest is a novel in-situ EC

synthesis approach for the formation of functionalized graphene (fG)-GO nanocomposite on a screen-printed electrode, SPE (Sharma et al, 2013). This approach combines good electronic properties of fG and reactive groups of GO for bioconjugation with biomolecules. SPE has been advocated and commercialized as disposable electrodes for a single use.

Fundamental aspects of bioconjugation

For IAs using a polystyrene-based MTP, graphene or its derivatives is simply coated into the containment vessel (well) to drastically increase the binding surface for the cAb. After binding to graphene, the cAb conformation is altered, depending on the surface chemical properties. In many cases, the cAb unfolds to expose hydrophobic regions that interact with the hydrophobic surface of graphene by passive adsorption. Modified graphene with a small number of ionic carboxyl groups results in a slightly ionic, hydrophobic surface. This feature is very important as biomolecules adsorb passively to surfaces through hydrophobic and ionic interactions. During the course of IAs, as several washing steps are required for the removal of unbound materials, a covalent binding provides a more stable biomolecule layer on graphene. In this case, GO or rGO with a large amount of oxygen functional groups including carboxyl groups must be used. The formation of amide bonds between amino-terminated biomolecules and carboxyl groups of modified graphene is a well-known strategy for bioconjugation. The most versatile crosslinker in aqueous preparation, 1-ethyl-3-(-3-dimethylaminopropyl) carbodiimide hydrochloride (EDC), reacts with carboxylic acid groups to form *O*-acylisourea, a carboxylic ester with an activated leaving group as the key intermediate (Vashist, 2012). The *O*-acylisourea intermediate then reacts with amines to give the desired amide. However, as *O*-acylisourea is not very stable, the preferred crosslinking chemistry is the use of EDC with *N*-hydroxysuccinimide (NHS) or N-hydroxysulfosuccinimide (Sulfo-NHS) (https://www.thermofisher.com/us/en/home/life-

science/protein-biology/protein-biology-learning-center/protein-biology-resource-library/pierce-protein-methods/carbodiimide-crosslinker-chemistry.html). Alternatively, carboxyl- or amino-containing molecules, e.g., perylene tetracarboxylic acid, poly(xanthurenic acid) and 1-aminopyrene, form stable complexes with graphene to enable covalent attachment. GNPs can also be modified to possess positively charged amine groups, which ionically couple to small negatively charged biomolecules. This surface is specifically designed to be used with bifunctional crosslinkers such as glutaraldehyde and carbodiimide to covalently couple to primary amines, thiols or carboxyls on Ab.

Considering Ab heavy chains located in a flexible region are joined by a disulfide bond, and like thiols, disulfides bind strongly to gold surfaces to form self-assembled monolayers (Grönbeck et al, 2000). Thus, graphene materials decorated with gold nanoparticles (AuNPs) can be conjugated with Ab by exploiting "well-known Au–S" interactions. Although the true nature of Au-S bonds is still unclear, the S-S bond is plausibly cleaved by the Au atoms on the Au surface upon its contact to thiolates, which in turn self-assemble on Au. The surface chemistry of Au colloids related to its negative surface charge and their interactions with functional amino acids has been described by Zhong et al. (2004). AuNPs with high surface-to-volume ratio and surface energy interact strongly with protein/enzyme to form a stable biolayer (Colvin et al, 1992).

CEA as a tumor biomarker

CEA is an important tumor biomarker for colorectal and some other carcinomas and its assay is widely accepted in the oncology practice as a useful and cost-effective tool for monitoring colon cancer after surgery. In the past, CEA was considered as an oncofetal antigen, expressed during the embryonic development and re-expressed only in cancer patients. Indeed, CEA is also

expressed in normal adults but it is produced in the colon and then disappears in feces. This cell surface glycoprotein plays a role in cell adhesion and in intracellular signaling. In colon cancer, the tumor cells have lost their polarity and CEA is distributed around the cell surface and eventually gets into the blood (Taylor and Black, 1985). CEA is a complex, highly glycosylated macromolecule (50 % carbohydrates) with a molecular weight of ~200 kDa (Hammarstrom et al, 1975), compared to 160 kDa for well-known glucose oxidase. Indeed, CEA in normal colon tissues has a broad band averaging at 200 kDa and a sharp band at 130 kDa. However, in cancer cells, only a single band at 170 kDa or lower has been observed, which is partly due to the modification of the glycosylation pattern of CEA by *N*-glycanase (Garcia et al, 1991). As a stable molecule, CEA is one of the most widely used tumor biomarkers and a prognostic indicator in clinical assays.

CEA should be minimal in the blood of healthy adults whereas an abnormal level of CEA may be a sign of cancer, especially colon and rectal cancer. Serum from patients with colorectal carcinoma often has higher CEA level than healthy individuals, ~2.5 μgL^{-1} (Ballesta et al, 1995). CEA may also be present in patients with pancreas, liver, breast, ovary, or lung cancer (Figure 2). Therefore, the CEA level measured before and after surgery indicates the surgical success and the prognosis of patient's recovery. CEA levels may also be measured during chemotherapy to evaluate the treatment progress and outcome.

Insert Figure 2 here

Immunosensing procedures for CEA

Among various commercial anti-CEA Ab obtained from mouse and rabbit, some Ab has specific reactivity with human, whereas others exhibit some cross-reactivity with monkey or

mouse/rat. Although graphene can be functionalized to form the covalent binding with the cAb, in most cases, graphene forms a nanocomposite with AuNPs, polymers, etc. to facilitate bioconjugation of the cAb, which forms an IMC with a target protein. Several procedures have also been attempted for the preparation of Au colloids including the popular route based on the reduction of hydrogen tetrachloroaurate(III) trihydrate by sodium citrate. In addition, a small molecule is added during the course of synthesis to control the size and distribution of AuNPs (Liu et al, 2003). Electrochemical deposition of AuNPs on the surface of an electrode, e.g. gold (Li et al., 2005) or GC (Majid et al., 2006), is another convenient and rapid way to increase the active surface area. The size and density of AuNPs on such electrodes are mainly controlled by the deposition time and the concentration of the Au salt solution besides the applied potential.

HRP, often used to label the dAb, binds to the Fc region of the capture antibody. This enzyme is a ~44 kDa glycoprotein with 6 lysine residues which are easily conjugated to a labeled molecule. Through the binding, HRP along with the heme iron Fe (III) quickly catalyzes the reduction of H_2O_2 in the presence of an electron mediator, e.g., tetramethylbenzidine (TMB) to produce a blue color solution (the resulting diimine), which can be read at 650 nm. The TMB-peroxidase pair is used extensively in ELISA with a colorimetric reader (Figure 3). Chloro-1-naphthol (4CN) (Hawkes et al., (1982) is another common substrate for this enzyme besides Prussian blue, Nile blue, toluidine blue, thionine, methylene blue, methylene green, ferrocene, hydroquinone, etc. For higher detection sensitivity, several fluorophores are also available for HRP: cyanine and fluorescein, nanocrystals of semiconductor material, and naturally fluorescent proteins such as phycoerythrin and allophycocyanin. The dAb can also be labeled with a dye, an electroactive species, QDs, NPs. However, IA with Au-labeled secondary antibodies has relatively low sensitivity and the signal is not permanent. Silver enhancement enhances the

detection sensitivity, which is equivalent to colorimetric alkaline phosphatase (AP) detection. AP is another labeled enzyme in immunoassays, but it is more expensive than HRP.

Insert Figure 3 here

In EC IMS, graphene can be used to modify other carbon material electrodes, ranging from graphite, carbon paste, GC, carbon nanotubes (CNTs) and even boron doped diamond. The electron mediator can be anchored together with the HRP-conjugated dAb on NPs to simplify the detection scheme. Of interest is nanoporous silver (NPS) with high specific surface area, electrical conductivity and adsorption capacity for a high loading of a suitable mediator (Liu et al, 2010). Thionine together with HRP significantly simplified improves the detection sensitivity of CEA (Figure 4). A similar approach using thionine and functionalized GO has been reported for the detection of phosphorylated p53 (S392), a potential biomarker in clinical diagnosis (Du et al, 2011). Alternatively, after binding to the cAb-CEA complex, the labeled HRP will be close contact with the electrode surface to catalyze H_2O_2 reduction and this approach has been frequently used in EC immunoassays. Without the enzyme, the graphene electrode does not exhibit high electrocatalysis for H_2O_2 reduction.

Considering label-free assays, electroactive molecules such as thionine and methylene blue (MB) form stable complexes with graphene/graphene derivatives via π-π stacking and ionic interactions. MB displays a quasi-reversible process with two-electron transfer with one proton (Tani et al., 2001) while its reduced form is colorless. MB shows peak absorption at 609 nm and 668 nm. Prussian blue is ferric ferrocyanide (Fe_4^{III} $[Fe^{II}(CN)_6]_3$) with alternating iron(II) and iron(III) located on a face of the cubic structure. Prussian blue is reduced to become Prussian

white (Fe_4^{II} $[Fe^{II}(CN)_6]_3$) with the loss of 4 electrons (Karyakin, 2001). If both the amines of thionine are dimethylated, the product tetramethylthionine is known as famous MB. Detailed electrochemistry of such dyes are well documented in the literature and deoxyribonucleic acid (DNA) electrochemistry with tethered MB has received considerable interest (Pheeney and Barton, 2012). The electron transfer from the excited MB to graphene is more efficient than to GO, owing to the different electrostatic attraction between the dye and graphene. In this context, MB, AuNPs and anti-CEA "layer-by-layer" self-assemble on a graphene-Nafion modified electrode (Figure 5). This is a label-free and simplified approach for the detection of CEA with high detection sensitivity (Li et al, 2011).

Insert Figure 4 here

Insert Figure 5 here

Investigation of fluorescence quenching of dyes by graphite oxide and graphene including a suggested mechanism can be found elsewhere (Liu et al, 2011). GO also quenches tryptophan or tyrosine containing peptides and proteins and electrostatic interaction plays an important role during quenching. Static quenching is the main mechanism, combined with Förster resonance energy transfer or dynamic quenching (Li et al, 2012). This is the rationale behind the use of GO together with a fluorescence dye in various IA formats. The binding of CEA to such a biofunctionalized surface exerts a strong steric effect, which reduces the electron transfer of the mediators. Of notice is the quenching behavior, known as fluorescence resonance energy transfer (FRET) (Loh et al, 2010) exhibited by GO. Neighboring fluorescent species to the graphitic carbon of GO are quenched by long-range "energy and electron" transfer (Swathi and Sebastian,

2008), which can be exploited for homogeneous assays of CEA and other biomolecules of interest. Chemiluminescence resonance energy transfer (CRET), however, occurs via non-radiative dipole-dipole energy transfer from a donor to an acceptor without an external excitation source. In the CRET platform with luminol, graphene is a better energy acceptor than GO, (Lee et al., 2012) as shown in Figure 6. Oxygenated functionalities are introduced in the graphite structure, which expand the layer separation and disrupt the sp^2 configuration. As a consequence, GO possesses a recombination of localized electron–hole pairs in a small sp^2 carbon domain within a sp^3 matrix. With luminol as the donor, the energy transfer efficiency is 72% for graphene and 36% for GO. Such a result is attributed to large Stokes shifts and long-range energy transfer efficiency of graphene (Lee et al, 2012) compared to GO. Molecules and nanomaterials with small Stokes shifts, i.e., low spectral separation of the acceptor emission from the donor emission should have a low energy transfer efficiency (Morales-Narvaez and Merkoci, 2012). Nevertheless, GO with a high planar surface, $\sim$ 2620 $m^2 g^{-1}$ (Stankovich et al, 2006), serves as an excellent platform for biomolecule loading and its potential use as an energy acceptor requires further investigation.

Insert Figure 6 here

Trends in technology for the detection of CEA

Albeit, color, fluorescence and EC measurements are often used to detect the binding event, of significance is a graphene-based CRET platform with remarkable detection sensitivity for homogeneous IA for C-reactive protein (CRP) (Lee et al, 2012). In this detection scheme, the anti-CRP Ab is conjugated to graphene nanosheets (with sulfonic acid groups) to capture and detect CRP at 1.6 ng mL^{-1} using the luminol/H_2O_2 chemiluminescence reaction catalyzed by

labeled HRP. CRET occurs via nonradiative dipole-dipole transfer of energy from luminol to graphene as mentioned previously. This efficient assay platform requires no removal of unbound antibody or phase separation and can be easily extended for other biomolecules of interest including CEA.

Electrochemiluminescence (ECL) is another new trend in particle-based IAs. An ECL label is tagged to NP bioconjugates, which are immobilized on the electrode surface. The most popular ECL label, tris(2,20-bipyridyl)ruthenium(II), ($[Ru(bpy)_3]^{2+}$), emits light when it reacts with ions, enzymes, tripropylamine (TPrA), etc. The reductant is oxidized at the electrode surface, which reacts with $[Ru(bpy)_3]^{2+}$ to yield $[Ru(bpy)_3]^{3+}$, which is measured by a photomultiplier, a charge-coupled device, etc. Magnetic NPs offer an ease of functionalization and enrichment of biomarkers from the complex mixtures, such as blood/serum. Together with ECL, this technology will find its widespread application to monitor the trace level of CEA or other pertinent biomarkers in whole blood.

A label-free technique based on surface plasmon resonance (SPR) also deserves a brief mention considering some recent developments in SPR biosensing with graphene modified sensing gold chips. A graphene sheet can be used to coat an Au SPR chip to increase the adsorption of biomolecules (Wu et al, 2010). GO can self-assemble on an SPR Au surface modified by 1-octadecanethiol to provide remarkable detection sensitivity for bovine serum albumin, down to 100 of pg mL^{-1} compared to 10 μg mL^{-1} for conventional SPR, i.e., about 100-fold more sensitive (Chiu et al, 2014). Indeed, protein A was conjugated on a gold surface of an SPR sensing chip and then coupled with anti-CEA Ab for detecting purified CEA with a limit of detection (LOD) of 0.5 ng mL^{-1} (Tang et al, 2006), well below the normal level in blood. With the graphene modified Au chip, the detection sensitivity should be significantly lower as

anticipated from the work of (Chiu et al, 2014). However, it is a formidable task to fabricate a multi-channel SPR and the cost of this instrument including disposable Au sensing chips could be another issue for its acceptance in clinical and hospital settings.

Direct electron transfer (DET) is another important feature in the construction of an efficient and "reagentless" electrochemical platform. Direct electron transfer (DET) to HRP is well established in contrast to glucose oxidase (GOx) where DET is highly unlikely (Liang et al. 2015). HRP is a very small enzyme (44 kDa) with the active heme group well exposed to the solution. It is also a very non-specific enzyme. In contrast, GOx is a 160 kDa protein with high substrate specificity. Although frequent claims of DET of GOx on graphene surface have been made (Shan et al, 2009), the evidence is not at all persuasive or even unlikely if the experiment is conducted in the absence of oxygen, a natural mediator of GOx (Liang et al, 2015). In brief, DET between HRP and an electrode is difficult because the active sites of HRP are embedded inside a thick protein shell. Therefore, a mediator is needed to shuttle electron from the active sites of the enzyme to the electrode surface. The development of mediator-free HRP enzyme based biosensor for H_2O_2 has emerged as exemplified by the DET of HRP on an AuNP modified carbon paste electrode (Liu and Ju, 2002), HRP–AuNP -GNP–silk fibroin modified GCE (Yin et al, 2009), ZnO (8-10 nm in diameter)-immobilized HRP (Xia et al, 2008), flower-like ZnO–AuNP–Nafion immobilized HRP (Xiang et al, 2009) and HRP on ZnO nanorods (Gu et al, 2009). These approaches improve the performance of the HRP-sensing platform for the reduction of H_2O_2 without the need for a mediator. The direct electron transfer is a big subject in bioelectrochemistry and beyond the scope of this review. However, this important feature has been investigated intensively for glucose oxidase with different detection schemes and strategies, ranging from sophisticated chemistry involving enzyme modification, nanowire, conducting

polymers, etc. to simple electrode modification (Bai et al, 2014). Such knowledge should be considered and adapted for the development of mediator-free HRP IAs.

Recently, different NPs have been known to exhibit intrinsic peroxidase-like activity. After the discovery of Fe_3O_4 (Gao et al, 2007), such behavior has been identified for ferromagnetic NPs (Shi et al, 2011), ceria oxide NPs (Asati et al, 2009), V_2O_5 nanowires (André et al, 2011), carbon-based nanomaterials (Song et al, 2010, Song et al, 2011), etc. In contrast to fragile HRP, NPs are very stable and retain their activity over a long period. They are not attacked by proteases and have greater resistance to pH, temperature, and extreme operating conditions. Consequently, NPs with intrinsic peroxidase activity will be integrated with graphene towards the development of simplified and robust IA platforms. Albeit Ab technology continues playing an important role in IAs, aptamers selected by *in vitro* selection have received considerable attention as affinity probes. Robust and highly stable aptamers can be designed with high affinity and specificity for any target including CEA. The combination of aptamers and peroxidase-like activity NPs could be envisioned as one of the best combinations. It should be noted that electrochemiluminescence of luminol is enhanced by ZnO nanoparticles, which forms the basis for a novel immune assay scheme for CEA (Cheng et al, 2012). However, the system is not completely free from enzyme since glucose oxidase is used to label the detection antibody to generate H_2O_2 in situ. Nevertheless, this enzyme is very specific for glucose which is also more stable than H_2O_2.

Most applications for the detection of CEA rely on laboratory-based instrumentation for color, fluorescence, chemiluminescence and even EC measurement. Cellphone (CP)-based technologies with smart applications are a new trend in bioanalytical applications. A compact colorimetric and fluorometric reader (Mudanyali et al, 2012), as well as a CP-based compact EC

sensing platform, have been reported (Lillehoj et al, 2013). Indeed, it is feasible for colorimetric readout from a 96-well microtiter plate (MTP) using a CP device (Vashist et al, 2015a, Vashist et al, 2015b) and the measurement of a full emission spectrum of any light emitter using a CP-based fluorimeter (Long et al, 2014, Yu et al, 2014). Together with graphene as a sensing interface, the CP-platform doubtlessly provides cost-effective mobile healthcare and personalized medicine with widespread applications for point of care testing (POCT) (Vashist et al, 2015c). The integration of screen printed graphene electrodes (SPGE) with an enhanced active area with a CP based electrical platform is appealing for POCT or doctor's office in remote areas. Graphene can be used to modify carbon-based screen printed electrodes and such products are also commercially available.

Insert Figure 7 here

Lastly, the clinical significance of CEA deserves a brief comment here as the clinician begin monitoring CEA levels in the cancer patients before the treatment to establish a baseline amount. The test will be repeated during and after treatment to assess changes over time. CEA levels often return to normal between one and four months after the tumors had been successfully removed. However, the CEA test is not useful in screening the general population for cancer. CEA monitoring in cancer patients, in particular, patients with colorectal cancer, is still controversial, which may vary from bimonthly monitoring to no monitoring in the surveillance setting (for stage I-III disease) and there are no clear guidelines in the metastatic setting. CEA monitoring in patients with other types of cancer, such as breast, lung, stomach, pancreas, ovary, bladder, thyroid and liver, is still unclear or debatable. Future endeavors may benefit from

evaluating CEA with other biomarkers to create a more precise index for cancer prognosis and recurrence. Thus, CEA might need to be measured with other tumor markers such as human epidermal growth factor receptor 2 (HER2, breast cancer cells)**,** prostate-specific antigen (PSA, prostate cancer)**,** cancer antigen 125 (CA 125, ovarian cancer cells), as well as CRP, a general biomarker for inflammation and infection. Conceptually, different capture antibodies can still be anchored on the same interface, however, second antibodies need to be conjugated with probes with different electrochemical or optical properties. As an example, carboxyl graphene sheets can interact strongly with toluidine blue or Prussian blue, followed by bioconjugation to serve as two different sensing probes (Figure 7). Indeed, this approach has been developed for the detection of CEA and alpha-fetoprotein as discussed in Table 2 (Chen et al, 2013). Finally, there is also a need to devise and validate prospective multiplexing strategies, enabling the precise determination of CEA in a sample together with such biomarkers. With the improved diagnosis, specific treatment can be offered to the patients to attain better treatment outcome.

References

Alwarappan, S., Erdem, A., Liu, C., Li, C.-Z., 2009. J. Phys. Chem. C 113, 8853-8857.

Alzari, V., Nuvoli, D., Scognamillo, S., Piccinini, M., Gioffredi, E., Malucelli, G., et al., 2011. J. Mater. Chem. 21, 8727-8733.

André, R., Natálio, F., Humanes, M., Leppin, J., Heinze, K., Wever, R., et al., 2011. Adv. Funct. Mater. 21, 501-509.

Asati, A., Santra, S., Kaittanis, C., Nath, S., Perez, J.M., 2009. Angew. Chem. Int. Ed. Engl. 48, 2308-2312.

Bai, Y.F., Xu, T.B., Luong, J.H.T., Cui, H.F., 2014. Anal. Chem. 86, 4910-4918.

Ballesta, A.M., Molina, R., Filella, X., Jo, J., Gimenez, N., 1995. Tumour Biol. 16, 32-41.

Brodie, B.C., 1859. Phils. Trans. R. Soc. Lond. 249-259.

Cao, Y., Yuan, R., Chai, Y., Liu, H., Liao, Y., Zhuo, Y., 2013. Talanta 113, 106-112.

Chen, X., Jia, X., Han, J., Ma, J., Ma, Z., 2013. Biosens. Bioelectron. 50, 356-361.

Cheng, Y., Yuan, R., Chai, Y., Niu, H., Cao, Y., Liu, H., et al., 2012. Anal. Chim. Acta 745, 137-142.

Chiu, N.F., Huang, T.Y., Lai, H.C., Liu, K.C., 2014. Nanoscale Res. Lett. 9, 445.

Chng, E.L.K., Pumera, M., 2011. Chem. Asian J. 6, 2899-2901.

Dreyer, D.R., Park, S., Bielawski, C.W., Ruoff, R.S., 2010. Chem. Soc. Rev. 39, 228-240.

Du, D., Wang, L., Shao, Y., Wang, J., Engelhard, M.H., Lin, Y., 2011. Anal. Chem. 83, 746-752.

Gao, L., Zhuang, J., Nie, L., Zhang, J., Zhang, Y., Gu, N., et al., 2007. Nat. Nanotechnol. 2, 577-583.

Garcia, M., Seigner, C., Bastid, C., Choux, R., Payan, M., Reggio, H., 1991. Cancer Res. 51, 5679-5686.

Geim, A.K., 2009. Science 324, 1530-1534.

Grönbeck, H., Curioni, A., Andreoni, W., 2000. J. Am. Chem. Soc. 122, 3839-3842.

Gu, B.X., Xu, C.X., Zhu, G.P., Liu, S.Q., Chen, L.Y., Wang, M.L., et al., 2009. J. Phys. Chem. B. 113, 6553-6557.

Hammarstrom, S., Engvall, E., Johansson, B.G., Svensson, S., Sundblad, G., Goldstein, I.J., 1975. Proc. Natl. Acad. Sci. 72, 1528-1532.

Han, J., Zhuo, Y., Chai, Y.Q., Mao, L., Yuan, Y.L., Yuan, R., 2011. Talanta 85, 130-135.

Hernandez, Y., Lotya, M., Rickard, D., Bergin, S.D., Coleman, J.N., 2009. Langmuir 26, 3208-3213.

Hu, K., Kulkarni, D.D., Choi, I., Tsukruk, V.V., 2014. Prog. Polym. Sci. 39, 1934-1972.

Huang, X., Ren, J., 2011. Anal. Chim. Acta 686, 115-120.

Hummers Jr, W.S., Offeman, R.E., 1958. J. Am. Chem. Soc. 80, 1339-1339.

Jia, X., Liu, Z., Liu, N., Ma, Z., 2014. Biosens. Bioelectron. 53, 160-166.

Jin, B., Wang, P., Mao, H., Hu, B., Zhang, H., Cheng, Z., et al., 2014. Biosens. Bioelectron. 55, 464-469.

Jung, Y.K., Lee, T., Shin, E., Kim, B.S., 2013. Sci. Rep. 3, 3367.

Karyakin, A.A., 2001. Electroanalysis 13, 813-819.

Kong, F.Y., Xu, M.T., Xu, J.J., Chen, H.Y., 2011. Talanta 85, 2620-2625.

Lee, J.S., Joung, H.A., Kim, M.G., Park, C.B., 2012. ACS Nano 6, 2978-2983.

Li, S., Aphale, A.N., Macwan, I.G., Patra, P.K., Gonzalez, W.G., Miksovska, J., et al., 2012. ACS Appl. Mater. Interfaces 4, 7069-7075.

Li, Y., Yang, W.-K., Fan, M.-Q., Liu, A., 2011. Anal. Sci. 27, 727-731.

Liang, B., Guo, X., Fang, L., Hu, Y., Yang, G., Zhu, Q., Wei, J., et al., 2015. Electrochem. Commun. 50, 1-5.

Lillehoj, P.B., Huang, M.C., Truong, N., Ho, C.M., 2013. LabChip. 13, 2950-2955.

Lin, D., Wu, J., Ju, H., Yan, F., 2014. Biosens. Bioelectron. 52, 153-158.

Liu, N., Ma, Z., 2014. Biosens. Bioelectron. 51, 184-190.

Liu, S., Tian, J., Wang, L., Li, H., Zhang, Y., Sun, X., 2010. Macromolecules 43, 10078-10083.

Liu, S.Q., Ju, H.X., 2002. Anal. Biochem. 307, 110-116.

Liu, Y.L., Male, K.B., Bouvrette, P., Luong, J.H.T., 2003. Chem. Mater. 15, 4172-4180.

Liu, Y., Liu, C.-Y., Liu, Y., 2011. Appl. Surf. Sci. 257, 5513-5518.

Loh, K.P., Bao, Q., Eda, G., Chhowalla, M., 2010. Nat. Chem. 2, 1015-1024.

Long, K.D., Yu, H., Cunningham, B.T., 2014. Biomed. Opt. Express 5, 3792-3806.

Morales-Narvaez, E., Merkoci, A., 2012. Adv.Mater. 24, 3298-3308.

Mudanyali, O., Dimitrov, S., Sikora, U., Padmanabhan, S., Navruz, I., Ozcan, A., 2012. LabChip. 12, 2678-2686.

Neto, A.C., Guinea, F., Peres, N.M., 2006. Physics World, November: 1-6.

Nuvoli, D., Valentini, L., Alzari, V., Scognamillo, S., Bon, S.B., Piccinini, M., et al., 2011. J. Mater. Chem. 21, 3428-3431.

Peres, N.M.R., Guinea, F., Castro, A.H., 2006. Phys. Rev. B73, 125411, DOI: 10.1103/PhysRevB.73.125411.

Pheeney, C.G., Barton, J.K., 2012. Langmuir 28, 7063-7070.

Pinto, A.M., Goncalves, I.C., Magalhaesa, F.D., 2013. Colloids Surfaces B: Biointerfaces111, 188-202.

Premkumar, T., Geckeler, K.E., 2012. Prog. Polym. Sci. 37, 515-29.

Rafiee, J., Mi, X., Gullapalli, H., Thomas, A.V., Yavari, F., Shi, Y., et al., 2012. Nat. Mater. 11, 217-22.

Samanman, S., Numnuam, A., Limbut, W., Kanatharana, P., Thavarungkul, P., 2015. Anal. Chim. Acta 853, 521-532.

Shan, C., Yang, H., Song, J., Han, D., Ivaska, A., Niu, L., 2009. Anal. Chem. 81, 2378-2382.

Sharma, P., Tuteja, S.K., Bhalla, V., Shekhawat, G., Dravid, V.P., Suri, C.R., 2013. Biosens. Bioelectron. 39, 99-105.

Shi, G.H., Cao, J.T., Zhang, J.J., Huang, K.J., Liu, Y.M., Chen, Y.H., Ren, S.W., 2014 Analyst. 139, 5827-5834.

Shi, W., Zhang, X., He, S., Huang, Y., 2011. Chem. Commun. 47, 10785-10787.

Song, Y., Qu, K., Zhao, C., Ren, J., Qu, X., 2010. Adv. Mater. 22, 2206-2210.

Song, Y., Wei, W., Qu, X., 2011. Adv. Mater. 23, 4215-4236.

Staudenmaier, L., 1898. Berichte der deutschen chemischen Gesellschaft 31, 1481-1487.

Stankovich, S., Dikin, D.A., Dommett, G.H.B., Kohlhaas, K.M., Zimney, E.J., Stach, E.A., et al., 2006. Nature 442, 282-286.

Sun, G., Lu, J., Ge, S., Song, X., Yu, J., Yan, M., et al., 2013. Anal. Chim. Acta 775, 85-92.

Swathi, R.S., Sebastian, K.L., 2008. J. Chem. Phys. 129, 054703.

Tang, D.P., Yuan, R., Chai, Y.Q., 2006. Bioprocess Biosyst. Eng. 28, 315-321.

Taylor, D.D., Black, P.H., 1985. J. Natl. Cancer Inst. 74, 859-867.

Vashist, S.K., 2012. Diagnostics 2, 23-33.

Vashist, S.K., Lam, E., Hrapovic, S., Male, K.B., Luong, J.H.T., 2014. Chem. Rev. 114, 11083-11130.

Vashist, S.K., Schneider, E.M., Zengerle, R., von Stetten, F., Luong, J.H.T., 2015a. Biosens. Bioelectron. 66, 169-176.

Vashist, S.K., van Oordt, T., Schneider, E.M., Zengerle, R., von Stetten, F., Luong, J.H.T., 2015b. Biosens. Bioelectron. 67, 248-255.

Vashist, S.K., Luppa, P.B., Yeo, L.Y., Ozcan, A., Luong, J.H.T., 2015c. Trends Biotechnol., DOI: 10.1016/j.tibtech.2015.09.001.

Wu, D., Guo, A., Guo, Z., Xie, L., Wei, Q., Du, B., 2014. Biosens. Bioelectron. 54, 634-639.

Wu, L., Chu, H.S., Koh, W.S., Li, E.P., 2010. Opt. Express 18, 14395-14400.

Xia, C., Wang, N., Lidong, L., Lin, G., 2008. Sens. Actuators B Chem. 129, 268-273.

Xiang, C., Zou, Y., Sun, L.-X., Xu, F., 2009. Sens. Actuators B Chem. 136, 158-62.

Yin, H., Ai, S., Shi, W., Zhu, L., 2009. Sens. Actuators B Chem. 137, 747-753.

Yu, H., Tan, Y., Cunningham, B.T., 2014. Anal. Chem. 86, 8805-8813.

Zeng, X., Bao, J., Han, M., Tu, W., Dai, Z., 2014. Biosens. Bioelectron. 54, 331-338.

Zhong, Z., Wu, W., Wang, D., Wang, D., Shan, J., Qing, Y., et al., 2010. Biosens. Bioelectron. 25, 2379-2383.

Zhou, M., Zhai, Y., Dong, S., 2009. Anal. Chem. 81, 5603-5613.

Zhou, Z.M., Feng, Z., Zhou, J., Fang, B.Y., Qi, X.X., Ma, Z.Y., et al., 2015. Biosens. Bioelectron. 64, 493-498.

Zhu, L., Xu, L., Jia, N., Huang, B., Tan, L., Yang, S, et al., 2013. Talanta 116, 809-815.

Table Legends

Table 1. Dispersion and solubility of graphene.

Table 2. Immunosensing procedures for CEA.

Figure legends

Figure 1. Schematic representation of (a) the layer-by-layer (LbL)-assembled graphene oxide (GO) multilayer array and (b) the aptamer-based protein sensing mechanism of the LbL GO multilayer array (Jung et al, 2013). Reproduced with permission from the Nature Publishing Group.

Figure 2. Carcinoembryonic antigen (CEA), a highly glycosylated cell surface protein of molecular mass about 180 kDa. It is found in the tissue of a developing fetus and cancer tumors. Not all cancers produce CEA, however, increased levels of CEA may be found in colorectal (colon), breast, liver, lung, ovary, pancreas, prostalemedullary thyroid carcinoma, and protate cancer. The pictures of various organs are obtained from Google.

Figure 3. Principle of "sandwich" immunoassays. Graphene or its derivatives can be integrated with AuNPs to serve as an immobilization matrix for the capture antibody (cAb). CEA from the assay sample forms an immunocomplex with the cAb and this binding event can be detected by a labeled antibody, known as the detection antibody or and the secondary antobody. The label is an enzyme, like horseradish peroxidase (HRP), a fluorescent tag including quantum dots (QDs), electroactive molecules, or metallic nanoparticles. In ELISA, the binding event is detected by the enzymatic reaction, e.g., hydrogen poeroxide is reduced by HRP in the presence of luminol to produce a chemiluminescence signal.

Figure 4. A detection scheme for the development of an electrochemical (EC) immunosensor. The capture antibody (Ab1) is immobilized on AuNP-decorated 3D-reduced graphene, whereas thionine, the electron mediator and the HRP-conjugated detetcion antibody (Ab2) are successively absorbed on nanoporous silver (NPS). DPV (differential pulse voltammetry) is applied to acquire high detetcion sensitivity (Sun et al, 2013). Reproduced with permission from Elsevier B.V.

Figure 5. LbL self-assembly of methylene blue (MB), AuNPs and anti-CEA on a graphene-Nafion modified electrode: (a) Formation of the graphene-Nafion nanocomposite film, (b) adsorption of MB, (c) formation of the AuNP monolayer, (d) anti-CEA Ab immobilization, (e)

bovine serum albumin (BSA) blocking, (f) CEA capturing (Li et al, 2011). Reproduced with permission from the Japan Society of Analytical Chemistry.

Figure 6. Chemiluminescence resonance energy transfer (CRET) between graphene nanosheets and chemiluminescent donors (Lee et al, 2012). CRET occurs via non-radiative dipole-dipole transfer of energy from a chemiluminescent donor to a suitable acceptor without an external excitation source. Immunoassay is based on a typical luminol/H_2O_2 (reducing oxygen species) chemiluminescence reaction catalyzed by HRP labeled to the detection anti-CEA Ab. Reproduced with permission from the American Chemical Society.

Figure 7. Simultaneous detection of CEA and alpha-fetoprotein (AFP) using two different electroactive probes (Chen et al, 2013). A: preparation of two different probes using toluidine blue (TB) and Prussian blue, anchored on carboxyl graphene sheets, respectively, together with immobilized anti-CEA (upper) and anti-AFP (lower). Bovine serum albumin (BSA) is used to block remaining reactive sites to prevent non-specific binding. B. Immobilization of capture CEA and AFP on the surface of a glassy carbon electrode (GCE), which is pre-modified with chitosan and gold nanoparticles. Reproduced with permission from Elsevier B.V.

Table 1.

A. Solvents and non-solvents for dispersion of graphene

Solvents	Acetate, acetone, 2-aminobutane, chloroform, dimethylformamide, ethanol, ethyl isopropanol, γ-butyrolactone, methyl ethyl ketone, *N*-methylpyrrolidone, toluene, tetrahydrofuran, and other polar solvents.
Non-solvents	3-Aminopropyltriethoxysilane (APTES), sodium dodecylbenzene sulfonate, poly(sodium styrene sulfonate), polyoxyethylene octylphenyl ether.
Small aromatic molecules containing hydrophilic groups via π–π interaction	1-Pyrenebuyrate, *p*-phenyl-SO_3H, methylene green, pyrene-1-sulfonic acid pyrene-1-sulfonic acid, sodium salt and 3,4,9,10-perylenetetra-carboxylic diimide bisbenzenesulfonic acid.

B. Solubility of graphene in the most promising solvents (Hernandez et al, 2009).

Solvents	Dispersion conc. (μg L^{-1})
Cyclopentanone	8.5 ±1.1
1,3-Dimethyl-2-imidazolidinone	5.2 ± 1.3
N-Methyl-2-pyrrolidone-(NMP)	4.7 ± 1.9
N-Ethyl-2-pyrrolidone	4.0 ± 0.7
N-Dodecyl-2-pyrrolididone	2.1 ± 1.1
Acetone	1.2 ± 0.4

Table 2.

Immunosensing procedure and its performance	Detection range (LOD)	References and other remarks
AuNP–decorated graphene composites are used to modify a GC electrode. HRP-anti-CEA Ab and HRP are successively adsorbed on the Au–GN modified GC electrode. *p*-hydroquinone is used as an electron mediator. Both the anodic and cathodic peak current responses decrease after the immobilization of HRP-anti-CEA, indicating the electron transfer between the electrode and the solution is hampered by the steric hindrance effect. The successive binding of HRP induces increased cathodic peak current corresponding to a decreased anodic peak current.	0.010 to 10 ng mL^{-1} (0.04 ng mL^{-1})	(Zhu et al, 2013) CEA in human serum samples are determined and validated by ELISA.
Three-dimensional macroporous AuNPs/graphene composites serve as the working electrode and the cAb is immobilized on AuNPs. Thionine, the electron mediator and HRP- conjugated dAb are sequentially absorbed on nanoporous silver. HRP reduces H_2O_2, whereas thionine is oxidized and recycled to its reduced form on the electrode surface to impart signal amplification.	0.10 to 80 ng mL^{-1} (0.04 ng mL^{-1})	(Sun et al, 2013) Good precision, stability and reproducibility. Applicable for clinical serum samples and in agreement with ELISA.
A cryogel consisting of graphene, AuNPs and chitosan are prepared on an Ag modified Au electrode. Ag acts as a redox mediator and the cAb is immobilized on AuNPs. The decrease in the Ag peak current obtained by cyclic voltammetry, reflecting the formation of the IMC to hinder the electron transfer, is proportional to the CEA concentration. The cryogel modified approach a 25-fold lower LOD than the non-cryogel counterpart.	1.0×10^{-6} to 1.0 ng mL^{-1} (2.0×10^{-7} ng mL^{-1})	(Samanman et al, 2015) The results obtained from serum samples are in agreement with enzyme linked fluorescent assay.
A GC electrode is modified by a nanocomposite consisting of AuNPs, thionine, and rGO. The anti-CEA Ab is immobilized on AuNPs. The decrease in the thionione peak current reflects the formation of an IMC complex. This complex acts as an insulating layer to block the electron transfer toward the electrode surface.	10-500 pg mL^{-1} (4 pg mL^{-1})	(Kong et al, 2011) Recovery experiments are performed by adding 40 to 200 pg mL^{-1} of CEA in human serum. The recovery ranges from 92.5 to 113 %.
Layer-by-layer (based on opposite-charged interaction) of MB as a redox probe, AuNPs and anti-CEA Ab are self-assembled on a graphene-Nafion nanocomposite film-modified electrode. Cyclic voltammetry confirms the oxidation and reduction peaks of MB. The measurement of CEA is conducted by differential pulse voltammetry and shows that the peak current decreases with the increasing concentration of CEA as expected from the formation of the IMC on the electrode surface.	0.5 to 120 ng mL^{-1} (0.17 ng mL^{-1})	(Li et al, 2011) The system is evaluated on several clinical samples and the obtained results agree well with those of ELISA.
A GCE is modified by a complex film of chitosan-ferrocene nano-TiO_2 and AuNP-graphene. The Au-graphene nanohybrid is formed on the complex by self-assembly. The anti-CEA Ab is anchored by a strong interaction between Au-graphene and the NH_2 groups of anti-CEA Ab. The synergistic effect	0.01 to 80 ng mL^{-1} (3.4 pg mL^{-1})	(Han et al, 2011) High sensitivity and long life time. Human serum samples are tested and

between AuNPs and graphene nanosheets results in good conductive response signals.		validated by ELISA.
A GC electrode is modified by AuNPs and Prussian Blue followed by the immobilization of the anti-CEA Ab. The assay is performed using HRP-conjugated anti-CEA Ab as the secondary Ab attached on the AuNP-graphene surface. Prussian blue acts as an electron mediator.	0.05-350 ng mL^{-1} (0.01 ng mL^{-1})	(Zhong et al, 2010) The results obtained from human serum samples are in agreement with the references values
A GC electrode is modified by a SWCNT-graphene composite and electrodeposited AuNPs. A sandwich protocol is used to generate amplified cathodic ECL signals using Pd and Pt NPs decorated rGO and glucose oxidase (GOD) labeled secondary Ab. GOD catalyzes glucose to produce H_2O_2 as a by-product, which reacts with luminol.	0.0001 -160 ng mL^{-1} (0.03 pg mL^{-1})	(Cao et al, 2013) The recovery ranges from 96 to 109% from the standard addition method (adding CEA in normal human serum samples.
A nanocomposite prepared by the self-assembly of ionic liquid (IL, 1-aminopropyl-3-methylimidazolium chloride) functionalized rGO and AuNPs via electrostatic interaction results in uniform AuNPs on the IL-rGO surface with high density. Based on a sandwich-type protocol, CEA and alpha-fetoprotein (AFP) are co-detected using two different tags: Prussian blue coated chitosan NPs and cadmium hexacyanoferrate NPs loaded with AuNPs. The detection is based on differential pulse vottammetry (DPV) using ferri/ferrocyanide as the probe.	0.01 to 100 ng mL^{-1} (0.01 ng mL^{-1} for CEA and 0.006 ng mL^{-1} for AFP)	(Liu and Ma, 2014) The results for both CEA and AFP are in agreement with ELISA. No non-specific adsorption and cross-talk are noticed.
The capture anti-CEA Ab is covalently immobilized on an electrochemically reduced GO/chitosan film layered on the surface of a GC electrode. The AuNP/mesoporous carbon foam (MCF) tag is prepared by in situ growth of Nanogold grown on carboxylated MCF (mesoporous carbon foam) serves as a tag, which is layered on the immunoconjugate to induce an Ag deposition process. The EC stripping signal of the deposited Ag is used to monitor the binding event. The nanocomposite-mediated Ag enhancement together with the graphene-promoted electron transfer results in high detection sensitivity.	0.05 pg mL^{-1} to 1 ng mL^{-1} (0.024 pg mL^{-1})	(Lin et al, 2014) The results obtained from clinical serum samples are within 12 % (relative error) from the commercial electrochemiluminescent tests.
A GCE is modified with chitosan and AuNPs to serve as a co-immobilization matrix for the capture anti-CEA and anti-AFP Ab. Two different sensing probes, toluidine blue (TB) for CEA and Prussian blue (PB) for AFP, are immobilized onto carboxyl graphene nanosheets (CGS), respectively via EDC/NHS activation. The detection antibody for each antigen is then bioconjugated to its corresponding modified CGS. DPV is applied to detect the electrochemical response peak of the two probes, before and after the formation of the two immunocomplexes.	0.5-60 ng mL^{-1} for both CEA and AFP (0.1 ng mL^{-1} for CEA and 0.05 ng mL^{-1} for AFP)	(Chen et al, 2013) The results obtained from clinical serum sample are in agreement with ELISA and there is no cross-talk between the two target biomarkers.
A nanocomposite is prepared from rGO/thionine/AuNPs and used for coating indium tin oxide sheets. The anti-CEA Ab is immobilized on thionine/AuNPs whereas the anti-AFP Ab is immobilized on Prussian blue/AuNPs. The decreased response current of thionine or Prussian blue is correlated well with the corresponding antigen concentration.	0.01-300 ng mL^{-1} for both CEA and AFP (0.650 pg mL^{-1} for CEA and 0.885 pg	(Jia et al, 2014) The results obtained from clinical serum samples agree with ELISA.

	mL^{-1} for AFP)	
A graphene platform is combined with magnetic beads (MaBs) and enzyme-labeled Ab-AuNPs. MaBs coated with the cAb is attached to graphene sheets by an external magnetic field to preserve graphene conductivity. The HRP-labeled dAb is immobilized on AuNPs. Graphene with high surface area serves as an electrical transducer. Cyclic voltammetry is used to probe the reduction of H_2O_2 by HRP (Fe^{3+}).	5-60 ng mL^{-1} (5 ng mL^{-1})	(Jin et al, 2014) LOD meets the clinical requirement but no real samples are tested by this approach.
A hybrid architecture of AuNPs-graphene, fabricated by reduction of $HAuCl_4$ and GO with ascorbic acid, serves as an excellent platform for Ab immobilization. ZnO NPs and glucose oxidase (GOx) functionalized graphene labeled secondary Ab are designed for this sandwiched ECL assay. The *in situ* generation of H_2O_2 is achieved by GOx in the presence of glucose, a co-reactant of the ECL-luminol reaction. The catalysis of ZnONPs to the ECL reaction of luminol–H_2O_2 system is exploited, not conventional HRP	10 pg mL^{-1} to 80 ng mL^{-1} (3.3 pg mL^{-1})	(Cheng et al, 2012) The analytical performance is evaluated by adding CEA to normal serum sample. The recovery ranges from 86 to 108 %.
In the diagnosis of cervical cancer, the detection of both CEA and squamous cell carcinoma antigen (SCCA) is required. Reduced GO-tetraethylene pentamine (rGO-TEPA) with amino groups is conjugated to the two capture Ab through amidation. Au@mesoporous carbon CMK-3 is synthesized and incubated with two detection Abs and two different redox molecules: neutral red and thionine. The sandwich structure detection scheme is based on the difference of the peak current of obtained for the two redox species before and after the IMC formation, i.e., absent and present of CEA and SCCA.	0.01-10.0 ng mL^{-1} (3.8 pg mL^{-1})	(Wu et al, 2014) The recovery of 5 ng mL^{-1} of CEA in serum samples ranges from 96-104 %. There is no cross-talk between CEA and SCCA.
A GCE is modified by tripetalous cadmium sulfide-graphene (CdS-GR) nanocomposites. The L-cystine film on the modified electrode is used for aptamer immobilization. The response signal is based on the ECL of cadmium sulfide-graphene (CdS-GR) nanocomposites as the acceptor whereas peroxydisulfate acts as the donor. Gold nanoparticles are assembled onto the L-cys film modified electrode for aptamer immobilization and ECL signal amplification. The decreased ECL intensity is correlated directly with increasing CEA concentration. Besides its role as an immobilization matrix, L-cystine also promotes the electron transfer, resulting in enhanced the ECL intensity.	0.01 to 10 ng mL^{-1} (3.8 pg mL^{-1})	(Shi et al, 2014) The recoveries of CEA in the human serum samples are 85 to 109.5 % with a relative standard deviation value of less than 3.4%.
A competitive photoelectrochemical platform is based on nanocomposites consisting of CdSe QDs (quantum dots) sensitized titanium dioxide decorated rGO. The CdSe/TiO_2-rGO nanocomposite is known to exhibit a high photovoltaic conversion efficiency. TiO_2–rGO hybrids assemble with mercaptoacetic acid wrapped CdSe (MPA–CdSe) QDs through electrostatic interaction to form CdSe/TiO_2–RGO a nanocomposite film. 4-chloro- 1-naphthol 4-CN is oxidized to B-4-CHD (benzo-4-chlorohexadienone) by HRP with H_2O_2 as the reductant. Insulating B-4-CHD is then absorbed on RGO	0.003 to 100 ng mL^{-1} (1.38 pg mL^{-1})	(Zeng et al, 2014) The CEA results from clinical serum samples agree with commercial turbidimetric immunoassay with a relative deviation of less than 11.2 %.

via π–π conjugation, which led to hinder the AA diffusion to the electrode surface for scavenging the holes. The synergic effect of HRP and B-4-CHD decreases the background signal, providing signal amplification (the light irradiation of 430 nm and the applied potential of 0 V. The photocurrent vs the CEA concentration plot is linear.		
A chemiluminescence (CL) detection scheme is based on aptamer-GO by capillary electrophoresis (CE) using CEA aptamer conjugated with HRP and GO. The CE is conducted using non-coating quartz capillary (60 cm long with an inner diameter of 75 μm). Without CEA, the CL signal obtained from the well-known luminol/H_2O_2 pair) is quenched by the HRP-aptamer adsorbed on GO leading to CL resonance energy transfer (CRET). In the presence of CEA, HRP-Apt forms a stable immunocomplex with this antigen and cannot be adsorbed stable on GO. The CL catalyzed by HRP-Aptamer-CEA complex is detected without CRET, and the CEA content is estimated by the CL intensity.	0.0654 to 6.54 ng mL^{-1} (4.8 pg mL^{-1})	(Zhou et al, 2015) Five positive and five negative clinical serum samples are evaluated. The results are in agreement with those obtained by a LIAISON chemiluminescent immunoassay system (DiaSorinS.p.A, Italy) using a standard CEA kit (DiaSorinS.p.A, Italy).

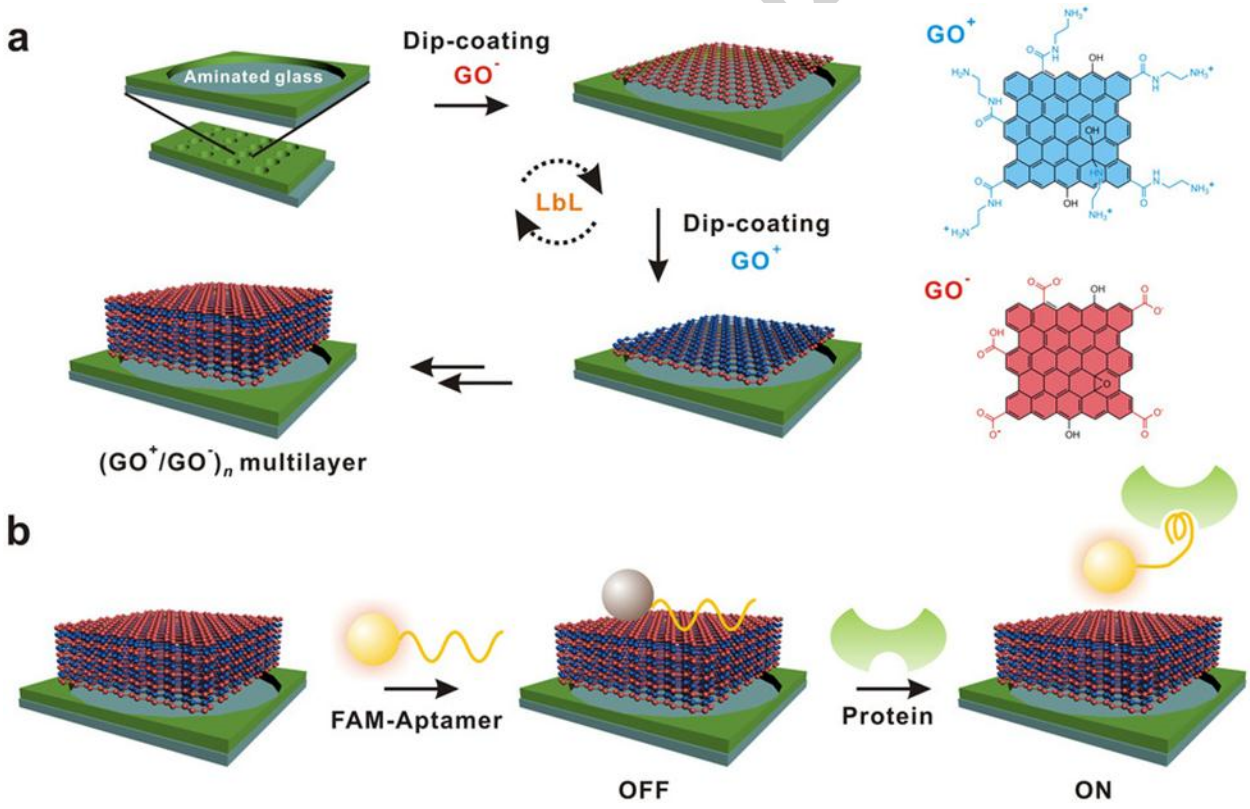

Figure 1

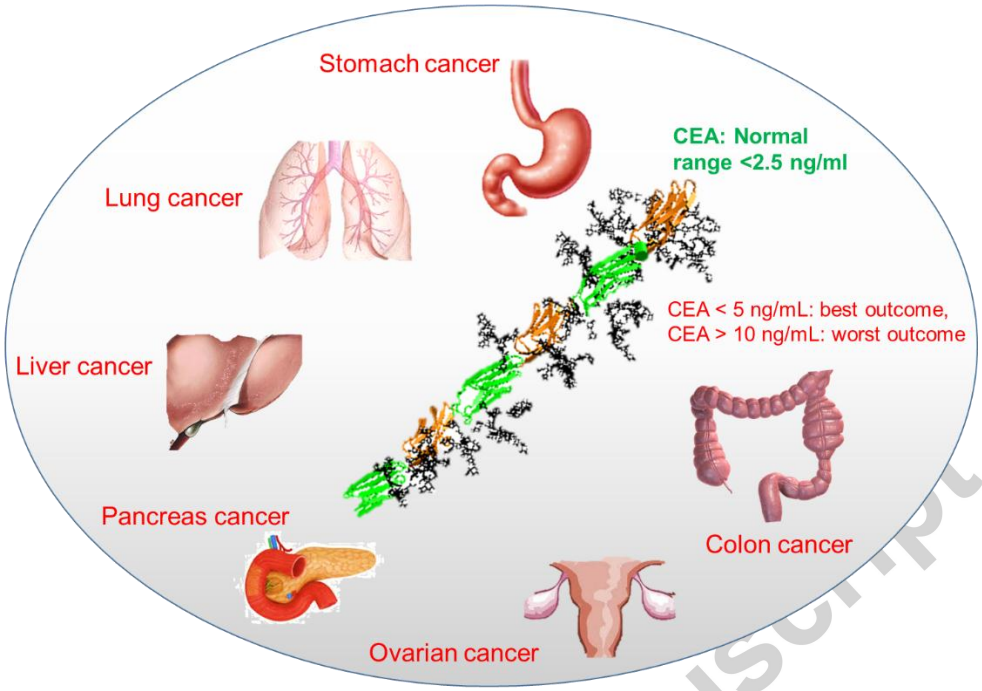

Figure 2

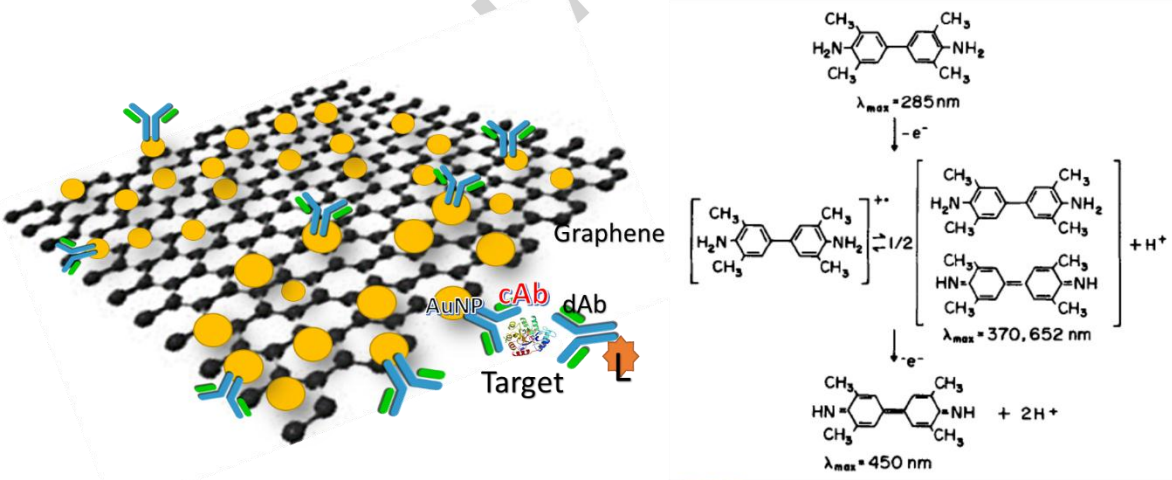

$H_2O_2 + HRP_{red} \rightarrow H_2O + HRP_{ox}$

$HRP_{ox} + Mediator_{red} \rightarrow HRP_{red} + Mediator_{ox}$

$Mediator_{ox} + 2H^+ + 2e^- \rightarrow Mediator_{red}$

Net reaction: $H_2O_2 + 2e^- + 2H^+ \rightarrow 2H_2O$

Figure 3

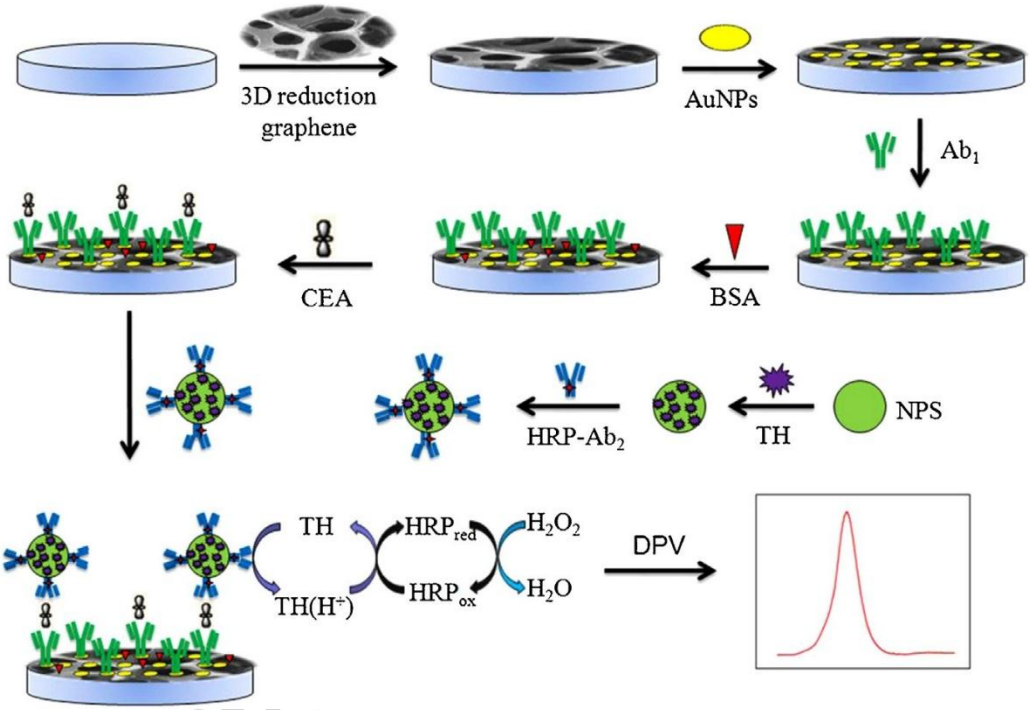
3D reduction graphene
AuNPs
Ab1
CEA
BSA
HRP-Ab2
TH
NPS
TH
TH(H+)
HRPred
HRPox
H2O2
H2O
DPV

Figure 4

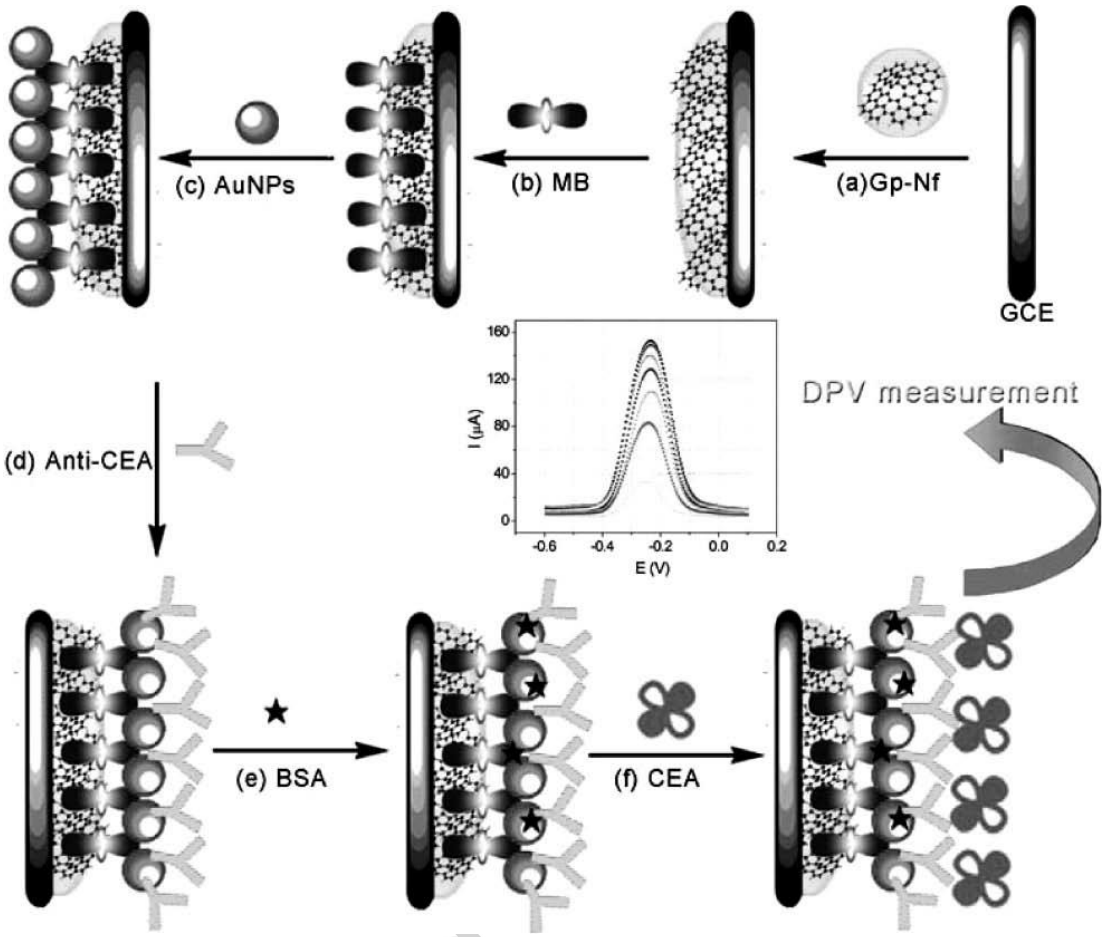

Figure 5

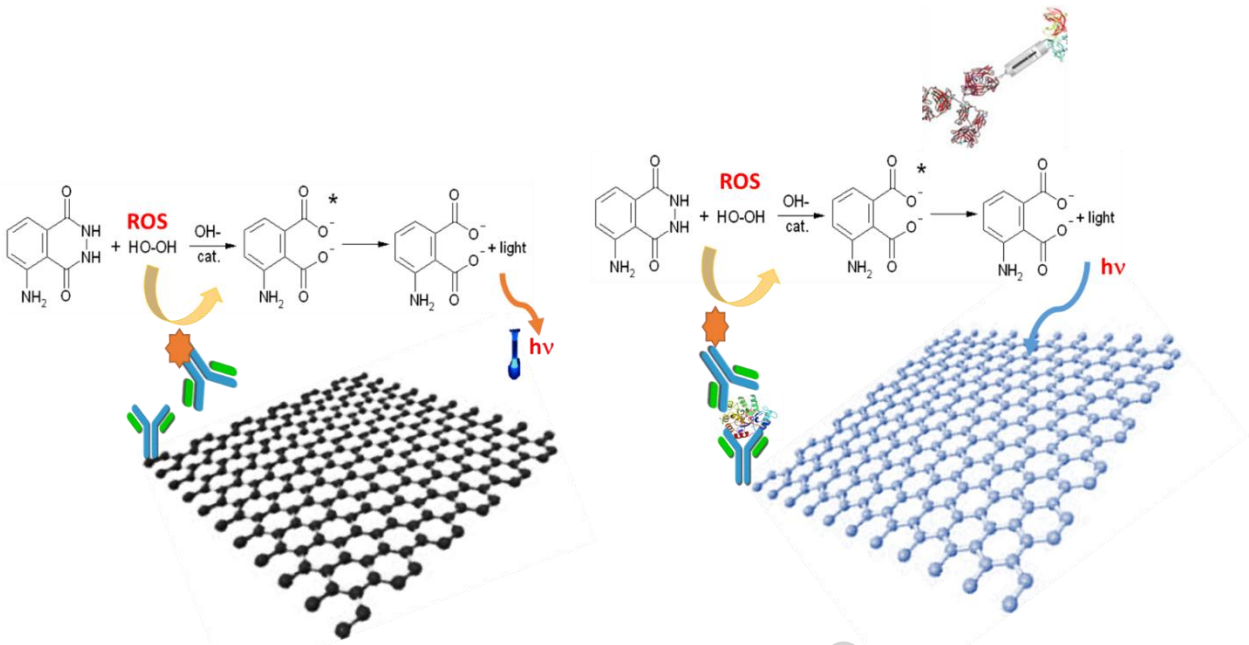

Figure 6

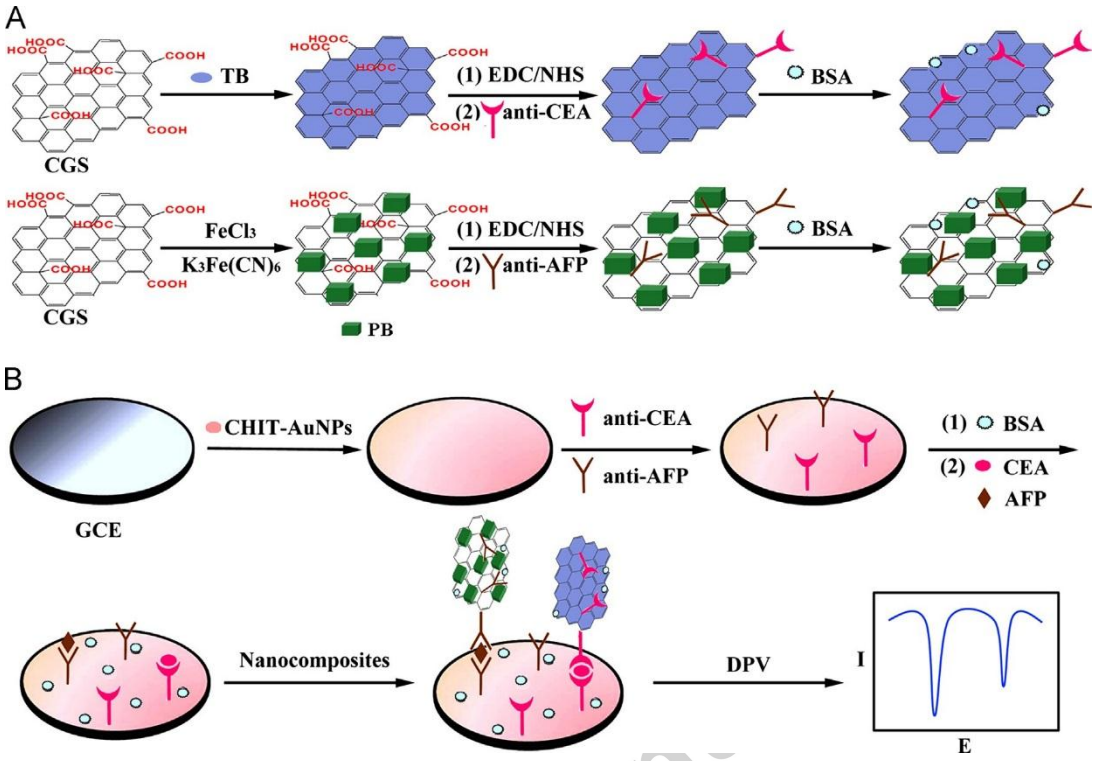

Figure 7

Highlights

- Graphene and nanocomposites based immunosensing of carcinoembryonic antigen (CEA)
- General chemistry and bioconjugation strategies for graphene and nanocomposites
- Clinical significance of CEA as a tumor biomarker and need for CEA detection
- Immunosensing procedures and trends in technology for the detection of CEA
- Advances in simultaneous detection of CEA with other pertinent biomarkers